We are IntechOpen,
the world's leading publisher of
Open Access books
Built by scientists, for scientists

6,900
Open access books available

185,000
International authors and editors

200M
Downloads

154
Countries delivered to

Our authors are among the

TOP 1%
most cited scientists

12.2%
Contributors from top 500 universities

WEB OF SCIENCE™

Selection of our books indexed in the Book Citation Index
in Web of Science™ Core Collection (BKCI)

Interested in publishing with us?
Contact book.department@intechopen.com

Numbers displayed above are based on latest data collected.
For more information visit www.intechopen.com

ACF Curing Process Optimization for Chip-on-Glass (COG) Considering Mechanical and Electrical Properties of Joints

Bo Tao, Han Ding, Zhouping Yin and Youlun Xiong
State Key Laboratory of Digital Manufacturing Equipment and Technology
Huazhong University of Science and Technology
P.R.China

1. Introduction

In the field of flat panel displays (FPD), packaging technology has significant influence on display performance. The electrical and mechanical interconnect between the liquid crystal displays (LCD) and its driver integrated circuit (IC) is a key issue that needs improvement to achieve finer pitch, easier assembly and greater connection reliability. With the decrease of the pixel size and the increase of pixel count for high-density LCD, the overall trend of the driver IC is packaged closer and closer to the LCD itself, even is onto the backside glass of the LCD. Bonding the driver IC chips directly to the glass substrate of the LCD panel might be a better choice when the pitch becomes less than 70–100 μm (Helge & Liu, 1998). Since the announcement by Citizen back in 1983 of a chip-on-glass (COG) driver assembly process for their LC pocket TV, many different types of COG assembly processes have been developed (Helge & Liu, 1998). In COG technology, the driver ICs are bonded directly to the indium-tin-oxide (ITO) traces on the glass without increasing the size of the panel, except for the finer bump pitch and smaller contact resistance, which can bring a significant reduction in the size of the FPD module. Because LCD is particularly heat sensitive and cannot withstand normal soldering temperatures, conductive adhesives are widely used to connect the driver IC to LCD. Usually, there are two different mechanisms used to cure the conductive adhesives, heat curing for thermosetting adhesives and UV curing for thermoplastic adhesives. Among them, heat curing appears to be most common. Nowadays interconnection using anisotropic conductive film (ACF) is the most major packaging method for production of FPD modules, to provide electrical conduction and mechanical adhesion between the driver ICs and the glass substrate with a high resolution, light weight, thin profile, and low power consumption (Myung & Kyung, 2006). Figure 1 presents a schematic illustration of a typical COG connection process using ACF.

ACF is a thermosetting epoxy impregnated with small amount of electrically conductive particles, which can be pure metals such as gold, silver, or nickel, or metal-coated ones with plastic or glass cores. During ACF curing, when the heat and force are applied, the conductive particles are trapped between the mating bumps of IC and substrate to provide electrical conductivity, and the adhesive matrix is used to provide the necessary electrical insulation, to protect the metallic contacts from mechanical damage, and to provide stable

adhesion. This arrangement allows ACF to conduct in z-direction, i.e. normal to the plane of adhesive film, while remaining insulation in the x–y plane due to the particles concentrated is far below the critical value to achieve percolation conduction. ACF has many distinct advantages over it counterparts. First, it is environment friendly, avoiding the toxicity and concerning from the lead and chlorofluorocarbon-based flux cleaners. Second, lower curing temperature is required that reduces joint fatigue and stress cracking problems. Third, it has higher flexibility and closer match in coefficient of thermal expansion (CTE) that enables a more compliant connection and minimizes failures. Furthermore, the smaller filling particle size facilitates finer line resolution, and the placement of adhesives is not critical. More recently, jointing technique based on ACF is playing an increasingly important role in the design and production of electronic packaging applications, such as the COG technique for LCD, flip-chip bonding of radio frequency chips, and so on (Yim, et al, 2005).
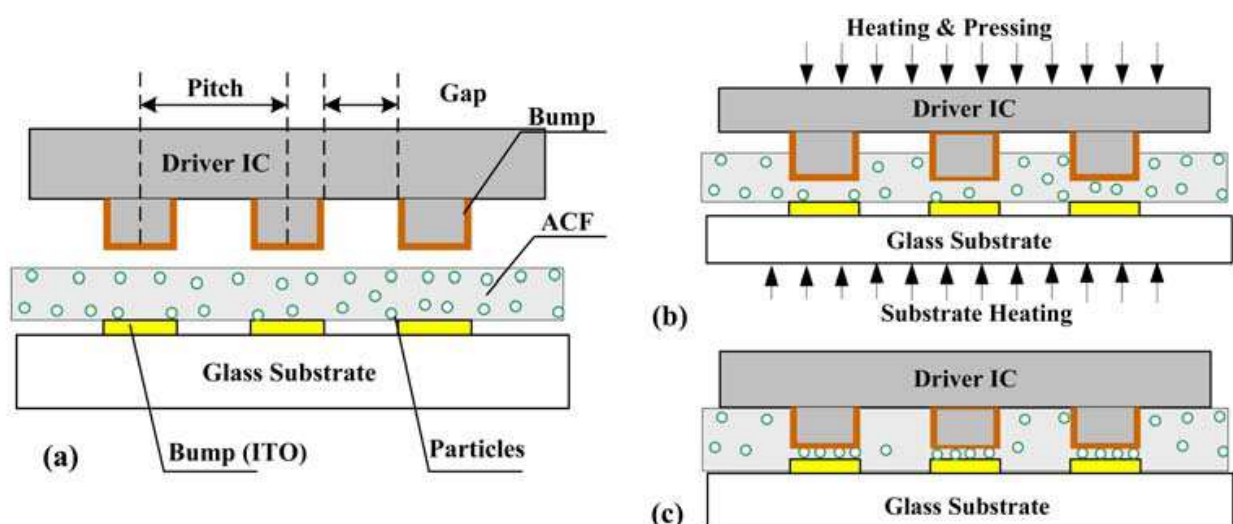

Fig. 1. A typical COG packaging process using ACF interconnection

The reliability of COG packaging is an important aspect in the electronics industry. It is found that the reliability is much dependant on the properties of the ACF (Lin & Zhong, 2008). Missing strong metal connection, ACF jointing usually has poor adhesion strength and unstable contact resistance, which are the two most critical reliability issues of ACF applications (Kim & Kim, 2008). High adhesion strength is a critical parameter of fine pitch interconnection that fragile to shocks encountered during assembly, handling and lifetime. During the curing process, voids are generated between the chip, adhesion and glass panel. These voids may affect the adhesion strength of the ACF, resulting in low reliability (Uddin, et al, 2004). Mechanisms to affect the stability of contact resistance include water absorption, electrochemical corrosion and metal oxidation, resulting in ever-increasingly unstable resistance through time, particularly under high temperature and high humidity conditions (Wu & Chau, 2002). These degradation mechanisms interfere with the contact resistance of ACF joints and hence limiting the ultimate electrical and mechanical performance of FPD module, which depends to a large extent on the curing conditions, including curing time, temperature, pressure, etc. Successful bonding involves the selection of proper bonding parameter, during which chemical reactions proceed to completion, in order to develop its strong adhesion strength and stable contact resistance.

During ACF bonding process, heat and pressure are applied concurrently to the component, and the conductive particles between an IC bump and a glass substrate pad change their

shape from spheres to ovoid to form the z-direction conduction paths. On the one hand, when heat is applied during bonding, the epoxy matrix of ACF is cured and becomes soft first and then rubbery. This transformation allows the ACF to flow, which in turn allows the conductive particles within to move and distribute themselves evenly throughout the ACF joints. When the curing process is completed, the ACF becomes hardened and the mobility of the conductive particles loses. A reliable electrical interconnect should have sufficient amount of conductive particles captured between the bump and pad, and they do not flow away after cured. The fluidity of the conductive particles during ACF bonding is strongly dependent on the curing temperature and time. Higher curing temperature and shorter time will limit the fluidity of particles and chemical reaction of epoxy, resulting in large and uneven contact resistance due to the less particles captured and their uneven distribution. Furthermore, inadequate chemical reaction will decrease the capability to endure the high hydrothermal impact during operations, which will speed the contact resistance shift (Hwang & Yim, 2008). On the other hand, the deformation amount of the conductive particles, determined by the amount of the pressure applied during the bonding process, has also a great influence on the contact resistance and adhesion strength of the ACF joints. Too much pressure will make the particle a larger deformation degree, meaning a larger recovery rate. When the external pressure is cancelled after cured, a larger residual stress will be present, due to the difference of the expanding fore of the deformed particles and the compressive force of the polymer matrix resin, which will speed the interface breakdown between ACF and IC or ACF and substrate. In fact, too much spread of the particles between adjacent bumps or pads, caused by too large pressure applied, will also increase possibility of short-circuiting. Whereas if the bonding force is too low, the particles may not be able to make contact between the connecting bumps and pads (Masahiro & Katsuaki, 2006). Moreover, in some cases an excessive pressure on bumps can cause glass breakage, so the bonding pressure imposed on the backside of the IC must be controlled precisely. Hence, to have a reliable ACF interconnection in a fine-pitched COG module, the thermo-compression bonding conditions need to be optimized except for the material properties of ACF.

Extensive studies have been done on the ACF bonding in past decades. However, most of them focus on certain bonding process parameter optimization, such as bonding pressure, temperature, time, and its correlations with the reliability of ACF joints subjected to various thermal, mechanical or environmental stresses. In fact, these bonding parameters not only influence the contact resistance of ACF joints but also determine their adhesive strengths greatly. Therefore, the electrical performance and adhesive strengths must both be considered to determine the optimum bonding parameters for reliability of interconnection from a systematic viewpoint of ACF curing reaction mechanism. Usually, the curing reaction of ACF is characterized by the curing degree of epoxy resin, defined as the fraction or extent to which the maximum possible cross links has been produced in a reaction. However, little work has been done to reveal the correlations of adhesion strength and contact resistance of flip chip with the curing degree of ACF matrix (Chung, et al, 2008). In the present work, the effect of different curing degrees on the electrical and mechanical properties of a typical ACF is studied through a systematic joints reliability evaluation method, and the optimum curing degree as well as its corresponding curing conditions for the given ACF is suggested to achieve highly reliable ACF joints, where the performance variations of the adhesion strength and contact resistance are considered simultaneously. The later sections are organized as follows. In section two, the degradation data of the

contact resistance of some ACF assemblies, bonded with several curing degrees, is collected during a standard high hydrothermal fatigue test. The resistance distribution of the ACF assemblies for each curing degree is verified and the distribution parameters are estimated respectively. In section three, a reliability analysis method based on the degradation data of contact resistance is adopted, and the reliability index as well as the mean-time-todegradation (MTTD) of ACF joints, as a function of the curing degree, is deduced, through which, the optimization curing degree is suggested. In section four, combining with the mechanism analysis and actual experiments, the curing kinetics model of the given ACF is built. Based on which, the optimum bonding parameters are suggested and are verified by way of actual ACF curing experiments. Finally, section five organizes this work and the value of this work is evaluated.

2. Degradation test and probability distribution analysis of ACF joints contact resistance

Investigators found that the worst environment for ACF joints was the thermal cycling and high hygrothermal (Wu & Chau, 2002). The contact resistance of ACF joints will become unstable through time, particularly under high temperature and high humidity conditions, where the mechanisms that affect the stability of contact resistance include water absorption, metal oxidation and electrochemical corrosion. The residual stress due to thermal compression during bonding, the oxidation of metal conductive bump and particles, hygrothermal expansion of adhesive and the CTE mismatch between components, were the main factors to result in the contact resistance increase of the ACF joints in the high hygrothermal environment. In this work, some high hygrothermal fatigue tests of ACF assemblies, bonded with several different curing degrees, are conducted under the high temperature (85°C) and high humidity (85%RH) conditions (so called 85/85 conditions), which are well known as the qualification standards throughout the electronic industry. The corresponding contact resistance is examined and is recorded. After that, the distributions to model the data collected are checked, and the distribution parameters are estimated respectively, which can be fitted as a function of the test time.

2.1 Experimental procedure
Four groups of ACF-based joints specimens were prepared with various curing degrees, which were achieved by controlling the curing time accurately and keeping the curing pressure 3N and temperature 170ºC unchanged for all specimens. In each group, there were four specimens. In the test, a thermosetting epoxy-based ACF was adopted, which contains Ag particles with an average diameter 3.5 µm and occupies 5% volume fraction or so. After that, all specimens were put into a chamber with the temperature 85°C and humidity 85%RH to reveal the contact resistance degradation, which will be used to evaluate the influence of curing degree on the ACF joints reliability. The contact resistance of all the specimens were measured and recorded every three days averagely, as listed in table 1.

2.2 Probability distribution of contact resistance degradation data
The contact resistance degradation data of each group specimens during the hygrothermal fatigue tests is appraised with the aid of the well-known two-parameter weibull distribution method. Figure 1 shows the weibull probability plots of each group specimens at various

Curing Degree	Test No.	Time of Contact Resistance Degradation Testing (Days)				
		0	3	6	9	12
80%	1	298	573	1337	NA*	1687
	2	218	958	1053	NA	1518
	3	273	855	1728	NA	1428
	4	168	NA	938	NA	1033
85%	1	278	550	735	NA	883
	2	225	705	740	NA	755
	3	215	752	1070	NA	1128
	4	195	763	885	NA	1143
90%	1	168	NA	758	NA	1100
	2	250	NA	878	NA	1263
	3	315	650	1037	NA	1363
	4	148	815	948	NA	1493
95%	1	373	958	NA	1185	1580
	2	205	488	NA	903	1278
	3	355	1270	NA	2288	2210
	4	138	290	NA	715	1350

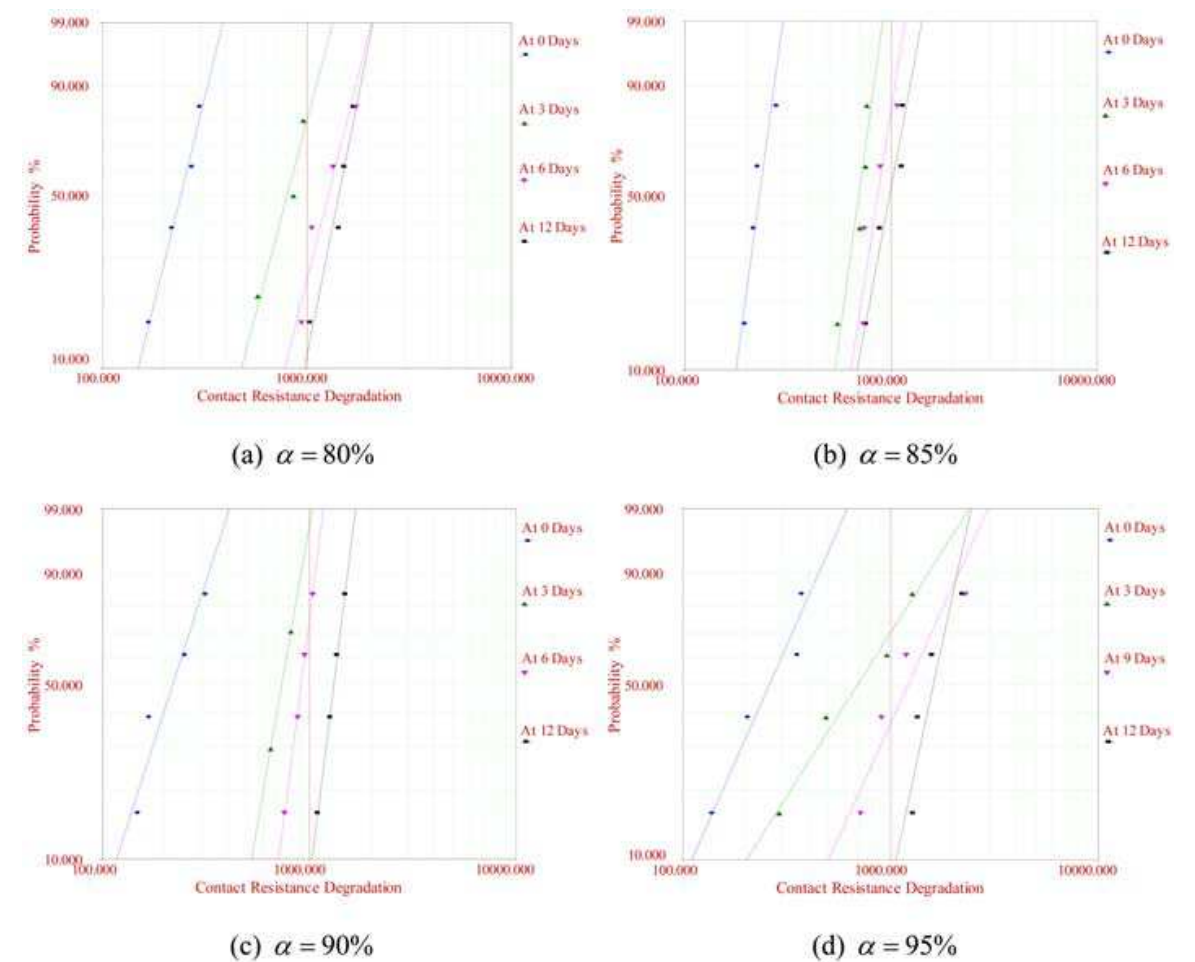Table 1. Contact resistances of specimens during the 85°C/85%RH hygrothermal test for various curing degrees (unit: mΩ)

Fig. 2. Weibull distribution of contact resistance degradation data for each group of specimens characterized by different curing degree α

observation time. From figure 2, it can be seen that for each group specimens, most of the data fall on the straight-line plots except for several occasional outliers. This suggests that the two-parameter weibull distribution is a reasonable candidate to model the contact resistance degradation data of ACF joints, so the probability density function (PDF) of the contact resistance of specimens can be given by:

$$f(x) = \frac{\beta}{\eta} \cdot \left(\frac{x}{\eta}\right)^{\beta-1} \cdot \exp\left(-\left(\frac{x}{\eta}\right)^{\beta}\right) \tag{1}$$

Herein, t is the hygrothermal testing time, β and η are the shape parameter and scale parameter of the weibull distribution respectively. Usually, both β and η are timedependent and can be expressed as a certain function of the hygrothermal testing time t. The shape and scale parameters of each weibull distribution plot, corresponding to different curing degree, are recorded, as listed in table 2.

Curing Degree	Distribution Parameters	Time of Contact Resistance Degradation Testing (Days)				
		0	3	6	9	12
80%	β	3.97	3.67	3.87	NA	4.92
	η (mΩ)	263.54	880.63	1390.69	NA	1536.46
85%	β	7.20	7.09	6.27	NA	5.21
	η (mΩ)	241.82	734.69	914.23	NA	1055.37
90%	β	3.00	5.59	7.60	NA	7.80
	η (mΩ)	246.64	785.62	957.74	NA	1378.58
95%	β	2.19	1.53	NA	2.14	4.53
	η (mΩ)	307.65	880.29	NA	1438.02	1740.97

Table 2. Weibull distribution parameters of each specimen group corresponding to figure 1

2.3 Estimation of the time-dependent distribution parameters

From table 2, it is found that the shape parameter keeps unchanged approximatively except for certain occasional outlier for each group, while the scale parameter all vary obviously with an incremental trend for each specimen group. Least squares fitting is used to model the data and the resultant time-dependent functions for each specimen group characterized by four different curing degree, namely 80%, 85%, 90% and 95%, are expressed by the equations (2) to (5) respectively, which are graphically shown in figure 3 correspondingly.

$$\begin{cases} \beta = 4.11 \\ \eta = 102.2 \times x + 481.2 \end{cases} \tag{2}$$

$$\begin{cases} \beta = 6.44 \\ \eta = 896.3 \times \exp(0.014 \times x) - 654.5 \times \exp(-0.395 \times x) \end{cases} \tag{3}$$

$$\begin{cases} \beta = 6.0 \\ \eta = 666.0 \times \exp(0.061 \times x) - 419.3 \times \exp(-1.153 \times x) \end{cases} \tag{4}$$

$$\begin{cases} \beta = 2.6 \\ \eta = 819.9 \times \exp(0.063 \times x) - 512.3 \times \exp(-0.514 \times x) \end{cases} \tag{5}$$

ACF Curing Process Optimization for Chip-on-Glass (COG)
Considering Mechanical and Electrical Properties of Joints
195

(a) $\alpha = 80\%$

(b) $\alpha = 85\%$
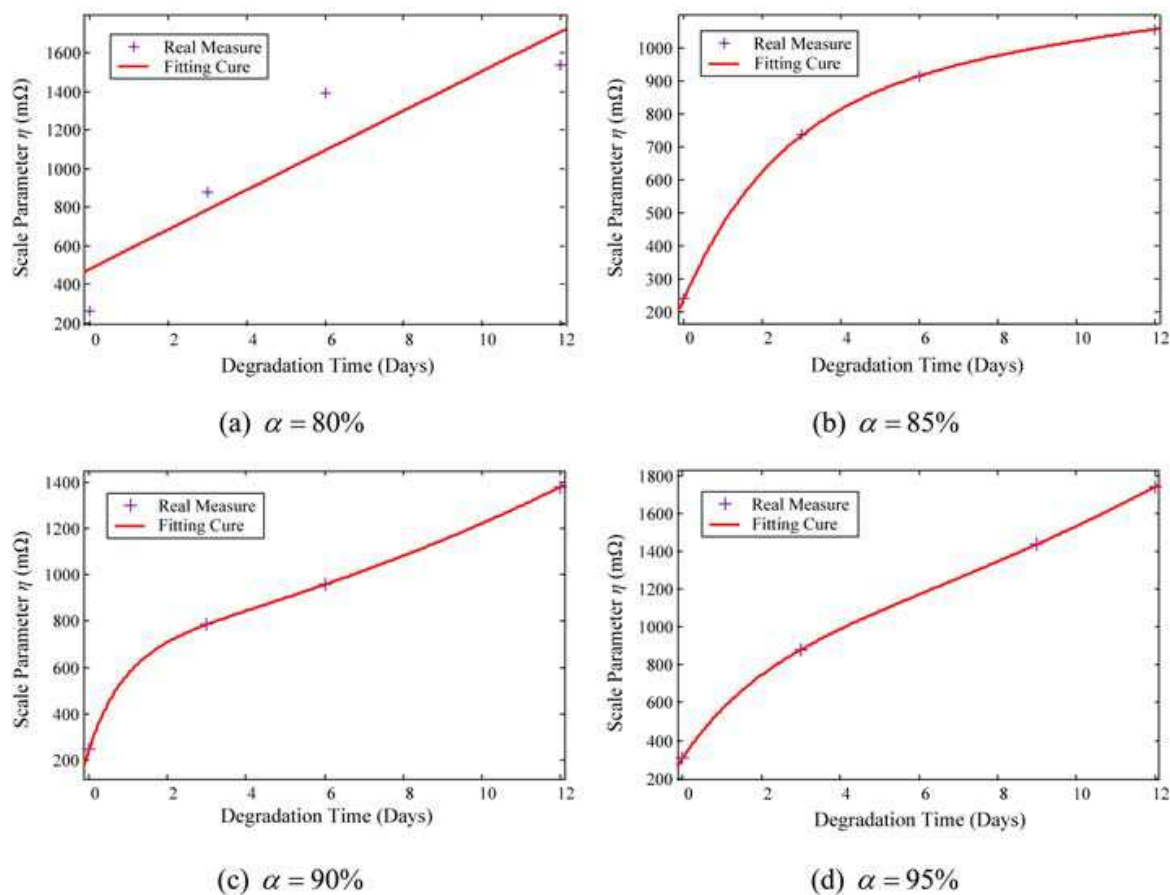

(c) $\alpha = 90\%$

(d) $\alpha = 95\%$

Fig. 3. Plots of weibull distribution shape parameters versus test time for each group specimens

As shown in figure 3, for each group, the scale parameter η increases with the increment test time t. That means the contact resistance of the ACF joints degrades in an exponential way except for the case where the curing degree is 80%. In the next analysis, all the shape parameters are characterized by the mean value of the test results.

3. Reliability analysis and curing degree optimization

Although the equations (2) to (5) are drawn from the given test data, it is still reasonable to conclude that the weibull distribution parameter η is the function of test time t while β is time-independent constant value for each specimen group. So submitting β and parametric $\eta(t)$ into the equation (1) yields the conditional probability density function of the contact resistance for each group at a given test time, written as:

$$f\left(x\,|\,t\right) = \frac{\beta}{\eta(t)} \cdot \left(\frac{x}{\eta(t)}\right)^{\beta-1} \cdot \exp\left(-\left(\frac{x}{\eta(t)}\right)^{\beta}\right) \tag{6}$$

Generally, the interfacial delamination of ACF bonding emerges during its application that can result in the failure of whole COG module. The failure criterion is usually defined as the resistance increase to certain threshold value, denoted by a constant d. Then the reliability function of the ACF joints at a specific time t for each group specimen is defined as:

$$\Re(d,t) = P(x \le d) = \int_0^d f(x \mid t) dx$$

$$= \int_0^x \left\{ \frac{\beta}{\eta(t)} \cdot \left(\frac{d}{\eta(t)} \right)^{\beta-1} \cdot \exp\left(-\left(\frac{d}{\eta(t)} \right)^{\beta} \right) \right\} dx = 1 - \exp\left(-\left(\frac{d}{\eta(t)} \right)^{\beta} \right). \tag{7}$$

From equation (7), it is found that the joints reliability is the function of time t and the failure threshold value *d*. Similarly, for each specimen group, the mean value function of the contact resistance at a specific time *t* is defined as:

$$\overline{x}(t) = \int_0^{+\infty} \{ x \cdot f(x \mid t) \} dx$$

$$= \int_0^{+\infty} \left\{ \beta \cdot \left(\frac{x}{\eta(t)} \right)^{\beta} \cdot \exp\left(-\left(\frac{x}{\eta(t)} \right)^{\beta} \right) \right\} dx = \eta(t) \cdot \Gamma\left(\frac{1}{\beta} + 1 \right) \tag{8}$$

Herein, $\Gamma(\bullet)$ is the Gamma function. Obviously, if the resultant mean value according to equation (8) equals to the failure threshold value *d*, the corresponding time *t* is the meantime- to-degradation of the specimen, denoted by MTTD, i.e.

$$d = \eta(MTTD) \cdot \Gamma\left(\frac{1}{\beta} + 1 \right) \tag{9}$$

Solving equation (9) will obtain MTTD value. Typically, for the ACF joints formed under the given curing degrees, namely 80%, 85%, 90% and 95%, β and $\eta(t)$ are given by the equation (2) to (5) respectively.

3.1 Time-dependent analysis of joints reliability

Substituting equation (2) to (5) into equation (7) respectively, the ACF joints' reliability functions, as a function of the hygrothermal test time for the four given curing degrees, are given respectively, by which the joints reliability at certain specific time *t* can be estimated and calculated if the resistance failure threshold value *d* is given. Two group curves of the reliability against the time for the given four group specimens according to two different failure criterions, i.e. 1000 mΩ and 1400 mΩ, are comparatively plotted together, as shown in the figure 4.
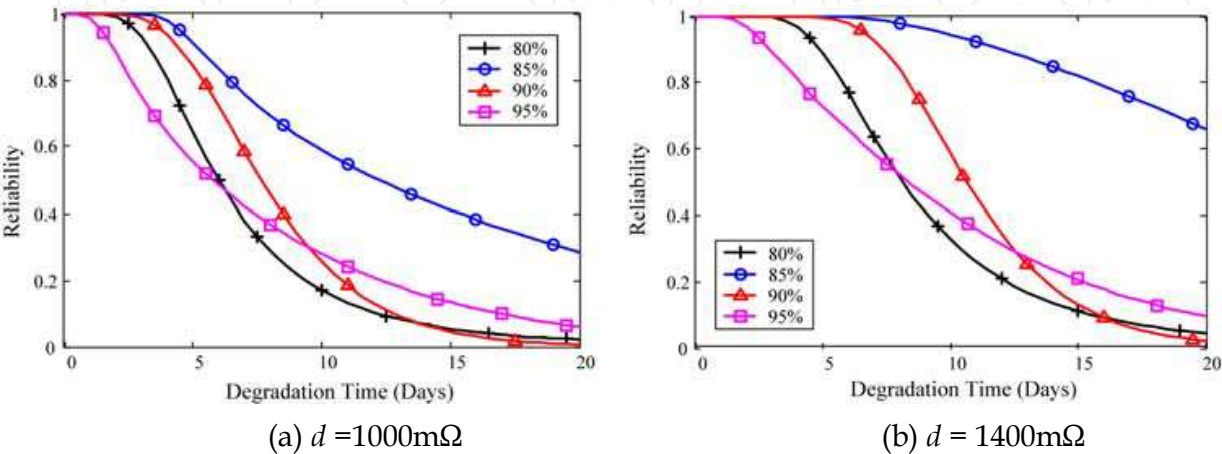

(a) *d* = 1000mΩ   (b) *d* = 1400mΩ

Fig. 4. Reliability curves of joints versus time for different failure criterion *d*

ACF Curing Process Optimization for Chip-on-Glass (COG)
Considering Mechanical and Electrical Properties of Joints
197

From figure 4, it is found that whichever the threshold value is used, the reliability of ACF joints reliability $\Re(d,t)$ versus hygrothermal test time t for each curing degree decreases monotonously while in different ways. This means that all the ACF joints, bonded under different curing degrees conditions, degrade by a single same or similar damage mechanism when suffering from same hygrothermal fatigue test. For the ACF joints tested, those, cured with a curing degree 85%, have a highest reliability than else obviously. That implies that the optimum curing degree is a certain middle value, near the 85%, in the range of 80% to 90%. For the ACF joints cured with other curing degrees, the reliability curves are interlaced to each other. For those with curing degree 95%, the reliability is lowest in the early time but the curve is flater than other two cases. That means that the ACF joints with high curing degree have a better endurance under the high hygrothermal environment.

3.2 Time-dependent analysis of joints resistance

Similarly, the mean resistance of ACF joints' can be quantitatively calculated by substituting equation (2) to (5) into equation (8) respectively. Clearly, from equation (8) it can be seen that the contact resistance of ACF joints is only correlated to the test time t. Numerical calculations are achieved for each group specimens, and the resultant resistance against hygrothermal test time t is graphically shown in figure 5. From figure 5, it is found that the resistance of all the ACF joints' increases monotonously with the increment of time t. The similar sigmoid shape except for the case 80% also implies that the ACF joints enough cured will degrade by a single same or similar mechanism under high hygrothermal environment. From figure 5, it is also found that the joints with the curing degree 85% have a lower contact resistance and a slower degradation rate than other specimens. That also implies that the optimal curing degree does exist near the 85% in the range of 80% to 95%. The optimum curing degree needs to be investigated further according to the mean time to degradation of joints in the following section.

3.3 MTTD calculation for given failure criterion

As mentioned above, the MTTD value of the joints can be estimated using equation (9) for a given failure threshold value of contact resistance. Usually, equation (9) is a highly nonlinear equation, and directly solving the optimal solution of MTTD for certain given threshold value is very difficult. Fortunately, figure 5 shows that there is a one-to-one relationship between contact resistance and fatigue time for each group specimens. That means that there will be only one optimal MTTD value for any given failure criterion. Herein, a numerical calculation method based an improved Golden Section Search arithmetic is used to calculate the desirable MTTD, described as follows:

1. Pick two large enough time values t_L and t_U that bracket the optimal *MTTD* range, and construct the goal function denoted by equation (9).
2. Calculate two interior values from $t_1 = 0.382 \times (t_U - t_L) + t_L$ and $t_2 = 0.618 \times (t_U - t_L) + t_L$, then calculate the corresponding $d(t_1)$ and $d(t_2)$.
3. Check if both the condition $abs(1 - t_1/t_2) \leq \varepsilon$ and $d(t_1) < d < d(t_2)$ are met, where ε is the convergence criterion and d is the resistance failure threshold value defined. If met, stop calculation and set MTTD $= 0.5 \times (t_1 + t_2)$, otherwise, turn to the step (4).
4. If $d > d(t_2)$, set $t_L = t_2$ with t_U unchanged. If $d < d(t_1)$, set $t_U = t_1$ with t_L unchanged. If $d(t_1) < d < d(t_2)$, set $_U = t_2$ and $t_L = t_1$. Repeat steps (2), (3) and (4) till the optimal estimation of MTTD or other calculation restriction is met.
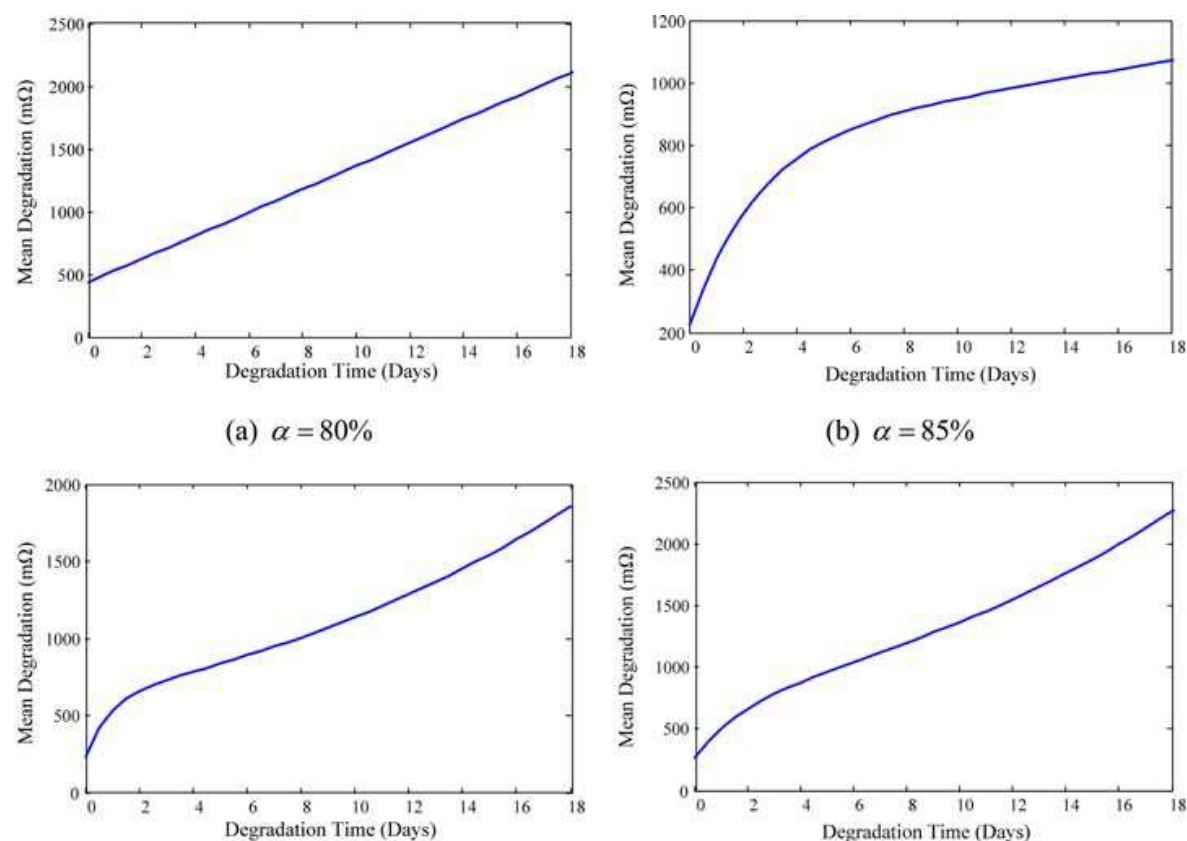
(a) $\alpha = 80\%$

(b) $\alpha = 85\%$

Fig. 5. Mean degradation value of contact resistance versus time for joints with varous cure degree

A C++ program agreeing with the above procedure is developed to compute the optimal MTTD value for certain given failure criterions, namely 1000 mΩ, 1100 mΩ, 1200 mΩ and 1400 mΩ, as listed in table 3.

Failure Criterion	Curing Degree			
	80%	85%	90%	95%
$D = 1000\text{m}\Omega$	6.07	14.85	8.25	5.19
$D = 1100\text{m}\Omega$	7.15	21.54	9.81	6.44
$D = 1200\text{m}\Omega$	8.23	27.75	11.24	7.70
$D = 1400\text{m}\Omega$	10.38	38.76	13.77	10.06

Table 3. MTTD value of ACF joints tested for different resistance failure criterions (unit: days)

3.4 Curing degree optimization analysis

To find the optimum value of curing degree, the influence of curing degree on the MTTD of the joints is analyzed. For a more reliable conclusion, least square fitting is used herein to model the data listed in table 3 for the four different failure criterions respectively, which are comparatively shown in fatigue 6.

From figure 6, it is found that for each failure criterion, the resultant MTTD value firstly increases and then decreases with the increment of the curing degree, and the maximum MTTD value of the ACF joints occurs at the curing degree 83% or so for each failure criterion. Although this conclusion is drawn from the given test data, it is still reasonable to

ACF Curing Process Optimization for Chip-on-Glass (COG)
Considering Mechanical and Electrical Properties of Joints
199

conclude that the optimum curing degree for the ACF tested is 83% or so, and the desirable range of the curing degree is 82% to 85% considering 95% confident interval. In fact, more failure criterions else have also been done, and same conclusions have also been drawn.
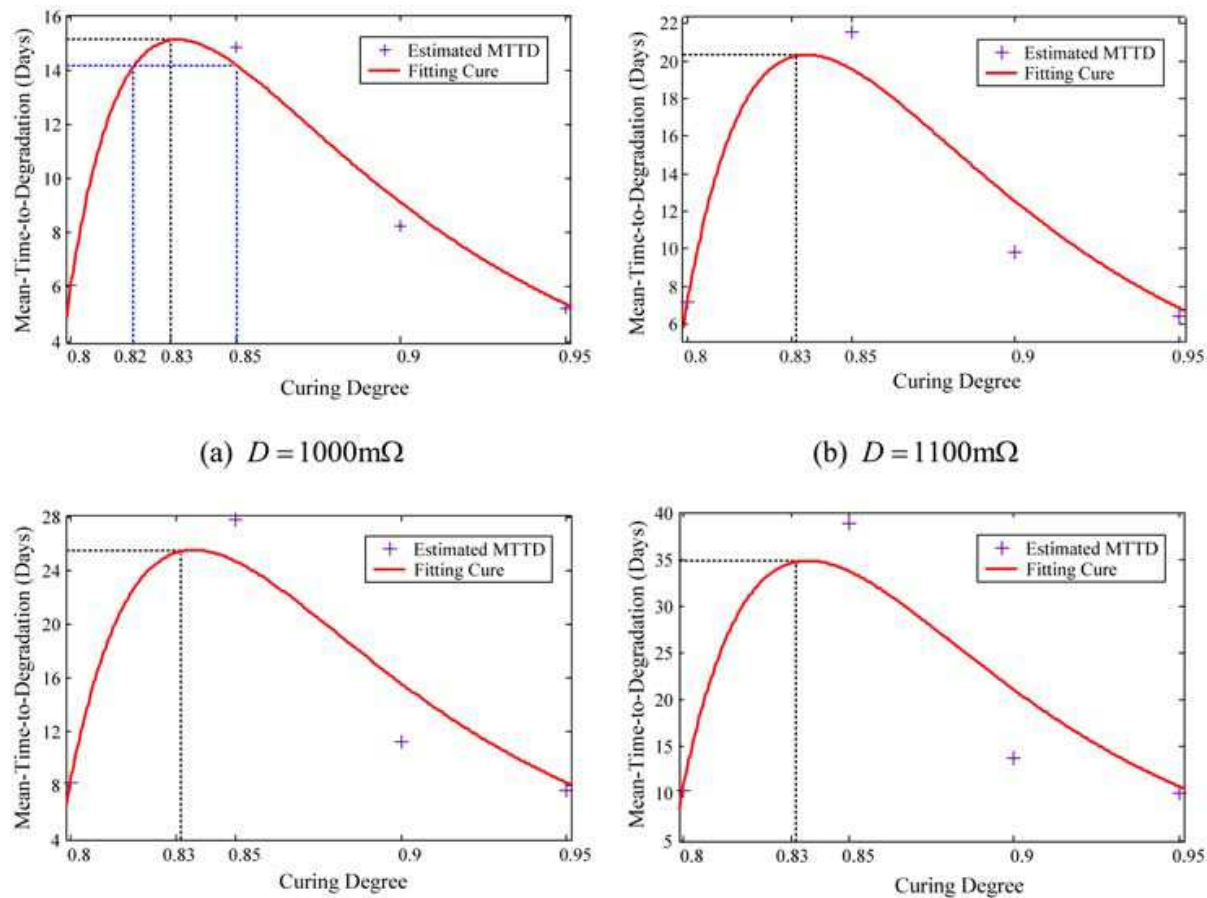

(a) $D = 1000\,m\Omega$ (b) $D = 1100\,m\Omega$

Fig. 6. MTTD value of joints versus curing degree for different resistance failure criterions

4. Curing parameters choice and optimization

Usually, the curing process of the ACF joints is achieved through controlling some key curing parameters, such as curing time, temperature and so on accurately, instead of controlling the curing degree directly. Therefore, we need to correlate the curing degree to those key parameters through curing kinetics modeling, by which the optimum curing parameters can be chosen for a given curing degree necessary.

4.1 Modeling for curing kinetics of ACF

To study cure kinetics of epoxy resin, several different methods have been proposed over the past decades, such as Fourier transform IR spectroscopy (FTIR), high pressure liquid chromatography (HPLC), nuclear magnetic resonance (NMR), differential scanning calorimeter (DSC), chemical titrations, and so on. Among them, DSC analysis is one of the best-known methods, which is mainly classified into two categories. One is isothermal test and the other is dynamic test. Both of them are based on the assumption that the exothermic heat evolved during the curing reaction is proportional to the extent of monomer conversion. That means that, for an ACF curing process, the measured heat flow dH/dt is proportional to the curing reaction rate $d\alpha/dt$. This assumption is valid if there are no other

enthalpic events except for chemical reactions occurring, such as evaporation, enthalpy relaxation, or significant changes in heat capacity conversion. Usually, the instantaneous change of the conversion rate is defined as:

$$\dot{\alpha} = \frac{d\alpha}{dt} = \frac{dQ/dt}{\Delta Q}.$$
(10)

Herein, ΔQ is the exothermic heat, expressed as heat per mol of reacting groups ($KJ \cdot mol^{-1}$) or per mass of materials ($J \cdot g^{-1}$). Usually, the curing kinetics equations of thermosetting materials are classified into two general categories: nth order and autocatalytic, which represents the overall process if more than one chemical reaction occurs simultaneously during curing (Chan, et al, 2003).

For thermosetting materials that follow nth order kinetics, the rate of conversion is usually proportional to the concentration of unreacted sections (Chan, et al, 2003), i.e.

$$\dot{\alpha} = k(1-\alpha)^n.$$
(11)

Herein, n is the reaction order, and k is the temperature-dependent rate constant given by the Arrhenius equation:

$$k = A \cdot \exp\left(-\frac{E}{R \cdot T}\right).$$
(12)

Herein, E is the activation energy, R is the gas constant, T is the absolute temperature, and A is the frequency factor. Equation (11) assumes that the reaction rate $\dot{\alpha}$ is dependent only on the amount of unreacted materials and the reacted sections do not participate in the remaining reactions. As such, a logarithmic plot of the equation (11) would result in a linear relationship, from which the reaction order can be estimated to the linear slope.

Autocatalyzed curing reactions, on the contrary, assume that at least one of the reacted sections will participate in the remaining reactions, and usually are characterized by an accelerating isothermal-conversion rate. The kinetics of autocatalyzed curing reactions is generally expressed by (Lee, et al, 1997):

$$\dot{\alpha} = \left(k_0 + k \cdot \alpha^m\right) \cdot (1-\alpha)^n.$$
(13)

Herein, m and n are the reaction orders. k_0 is the initial rate constant and is zero if no reactions occur at initial time. k is the temperature-dependent rate constant given by the equation (12). For autocatalytic reactions, at least two reaction orders, i.e. m and n, are needed to be determined. Boey and Qiang (2000) propose a numerical method to estimate the parameters that depend on the extent of reaction at the exothermic peak as well as the rate of the reaction at the peak. Usually, to simplify the calculation, the total reaction orders are assumed to two, i.e. let $m+n= 2$. Thus, the coefficients of the kinetics equation modeled by equation (13) can be estimated from the following equation group:

$$\begin{cases} \alpha_p = \dfrac{m}{m+n} \\ m+n = 2 \\ \dot{\alpha}_p = \dfrac{k \cdot m^n \cdot n^m}{(m+n)^{(m+n)}} \end{cases}.$$
(14)

Herein, α_p and $\dot{\alpha}_p$ are the curing degree and curing rate correspondingly at the exothermic peak, which can be easily obtained from the DCS thermogram.

It should be mentioned that in order to model the curing kinetics, it need to check the curing reaction of ACF given, nth order or autocatalytic. For the former, equation (11) indicates the maximum curing rate occurs at the time zero, while the maximum curing rate occurs at a certain middle time during the cure for the latter, which typically reaches its maximum between 20% and 40% conversion. Usually, the criterion mentioned here are used to check the curing kinetics of the undergoing reactions is nth order or autocatalytic. Whichever the kinetic model is adopted, the activation energy E and frequency factor A for the cure process must to be calculated. There are two different methods to estimate them according to the DSC test method adopted. For the isothermal DSC test, they can be estimated from the linear logarithm plot of the Arrhenius equation based on the isothermal curing test data. For the dynamic DSC test, the estimation of the activation energy and frequency factor can be achieved through the well-known Kissinger equation, as:

$$\ln\left(\frac{\beta_i}{T_{pi}^2}\right) = \ln\frac{A \cdot R}{E} - \frac{E}{R} \cdot \frac{1}{T_{pi}} \tag{15}$$

Herein, the subscript i is the specimen number, β is the heating rate and T_p is the peak temperature of reaction curve. Equation (15) indicates that there is a linear relationship between $\ln(\beta/T_p^2)$ and $1/T_p$. If the least square linear fitting is met, then E and A can be estimated from the slope and intercept of the linear plot fitted.

4.2 Coefficients estimation of curing kinetics

The estimation of the coefficients for the curing kinetics aforementioned is achieved through a group of dynamic DSC experiments, where a thermosetting epoxy-based ACF was tested using a DSC with a computerized data acquisition system in this study. The ACF contains Ag particles with an average diameter 3.5 μm and occupies 5% volume fraction or so. Some dynamic DSC tests were performed from 80°C to 180°C with four different ramp rate, namely 20°C/min, 15°C/min, 10°C/min, 5°C/min, during which, the rates of heat generation as a function of the temperature and time were recorded correspondingly. The plots of the dynamic DSC scans are shown in figure 7 and the resultant data were listed in table 4.

β (K•min^{-1})	T_p (K)	$\ln(\beta/T_p^2)$	$\ln\beta$ (K/sec)	$1/T_p$ (×10^{-3}K^{-1})
5	379.32	-10.267	-2.488	2.636
10	389.85	-9.629	-1.795	2.565
15	396.14	-9.255	-1.386	2.524
20	400.43	-8.989	-1.099	2.497

Table 4. Dynamic DSC data of ACF tested

From figure 7, it is found obviously that the larger the heating rate is, the sharper the curve does be. That means the curing process of the ACF is quickened with the increase of the heating rate. The calorimetric curve of figure 7(a) was integrated in order to obtain the integral curing curves, indicating the time dependence of the curing degree using a digital integral method. Herein, the curing degree was estimated by the division of the cumulative

heat at a certain time ΔQ_t over the total exothermic heat ΔQ of the curing process, as shown in figure 8. The zero-initial sigmoid shape of the curves means the maximum curing rate occurs at certain middle time of the overall cure process, which reveals that the undergone cure process follows an autocatalytic mechanism, and equation (13), keeping k_0 zero, will be adopted to model the cure kinetics of the ACF.
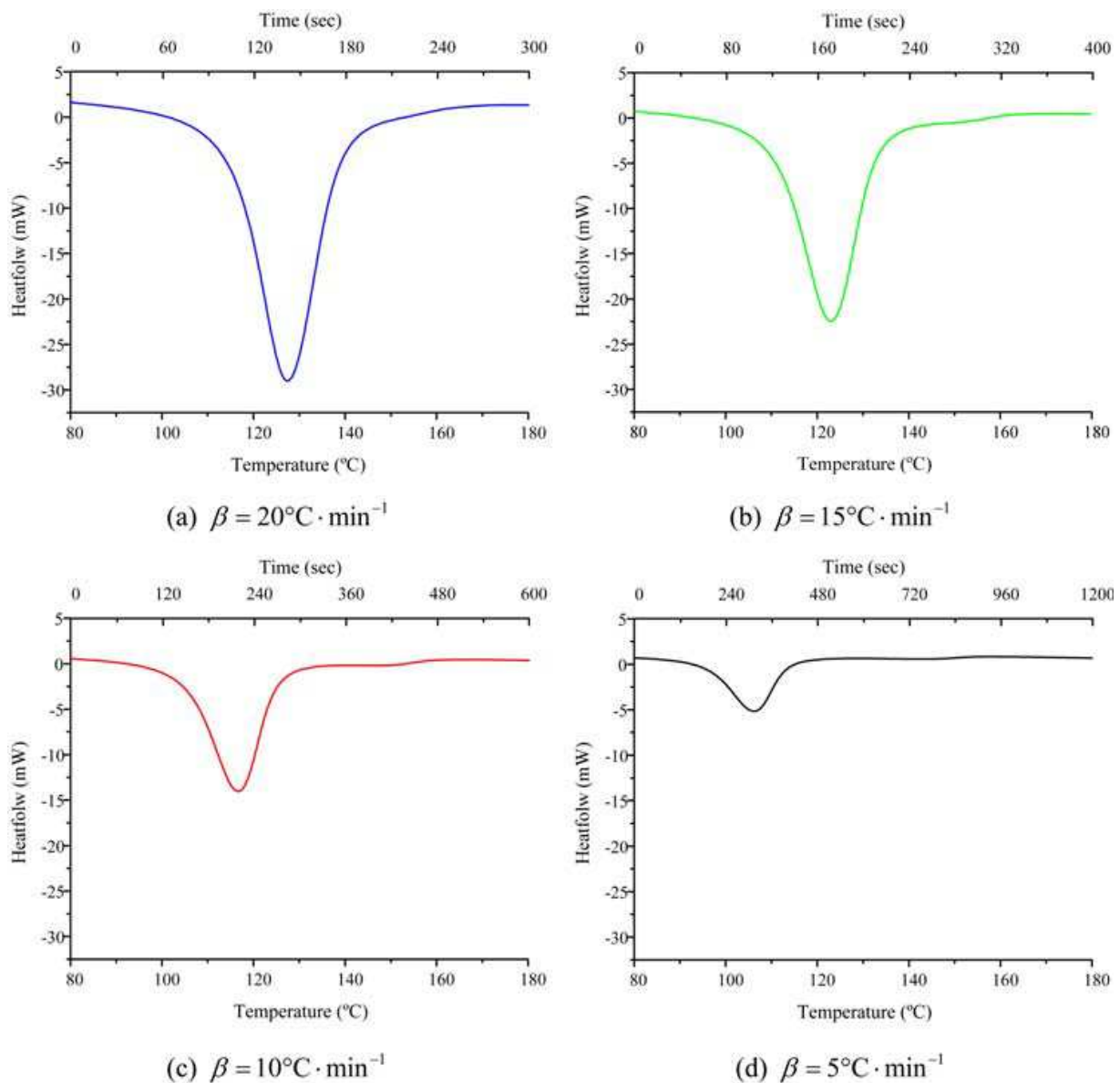

Fig. 7. Dynamic DSC plot of ACF for different heating rate

From the DSC thermograms, as shown in figure 7(a) and figure 8, the total exothermic heat ΔQ of the curing process is 1758.9 mJ and the cumulative heat ΔQ_t at the exothermic peak time is 935.4 mJ. Therefore, the cure degree at the exothermic peak, namely α_p, are 0.53. Taking it into equation (14), and the resultant coefficients m and n are 1.06 and 0.94 respectively.

Next, the activation energy E and frequency factor A will be estimated through Kissinger equation. Test data listed in table 4 is used to model the relationship of $-\ln(\beta/T_p^2)$ and $1/T_p$, and it is found that they follow a linear relationship with an ultra-high regression index 1.0,
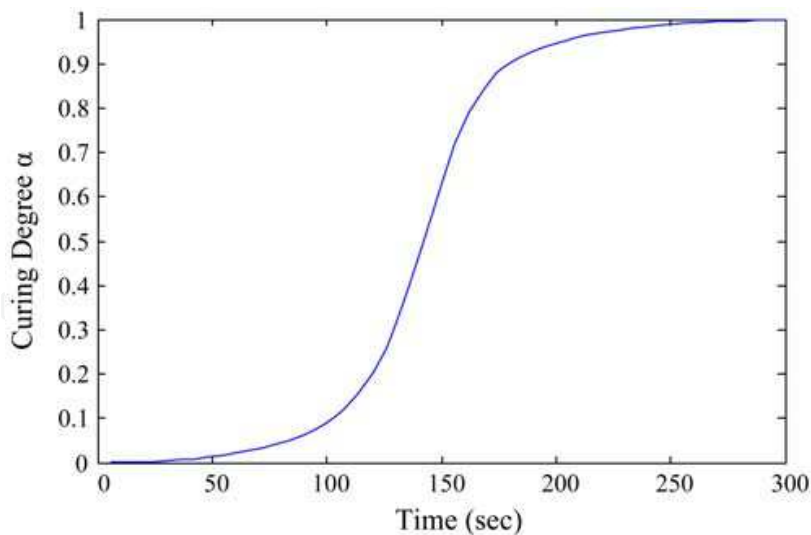
Fig. 8. ACF curing degree versus time under constant heating rate ($20°\,C\cdot min^{-1}$)

or so, as shown in figure 9. From the linear plot, the slope and intercept are found to be 9156.12 and -13.86. From equation (15), we can get the following equation group:

$$\begin{cases} \dfrac{E}{R} = 9156.12 \\ \ln\dfrac{A\cdot R}{E} = 13.86 \end{cases} \qquad (16)$$

Let the gas contast R is 8.314 J•mol^{-1}•K^{-1}, solving the equation group (16) can get that the activation energy E is 76.12kJ•mol^{-1} and frequency factor A is $1.60×10^8$ sec^{-1}.
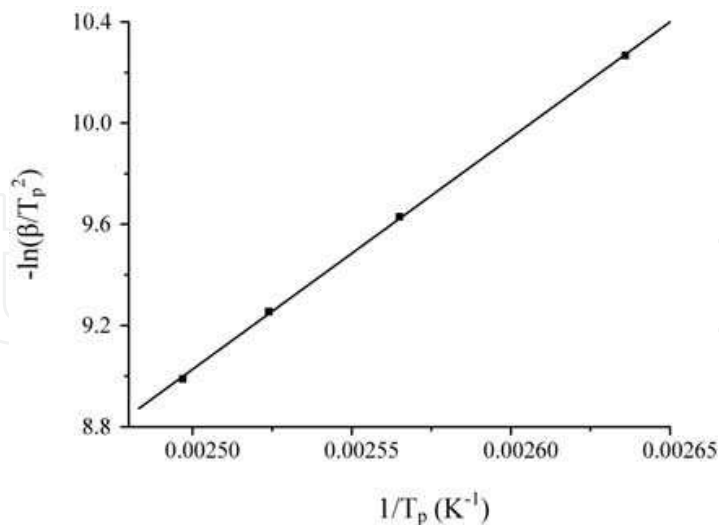
Fig. 9. Curve of $-\ln(\beta/T_p^2)$ versus $1/T_p$ for the ACF tested

4.3 Choice of curing parameters

Usually, there are mainly two curing patterns. One is the isothermal curing and the other is the non-isothermal curing. For the isothermal curing process, the function of the curing

degree versus curing time, for a certain curing temperature, can be obtained by directly integrating equation (13), which can be rewritten as the following form:

$$\frac{d\alpha}{\alpha^m \cdot (1-\alpha)^n} = A \cdot \exp\left(-\frac{E}{R \cdot T}\right) dt .$$
(17)

By taking the integral firstly and then the natural logarithm, the equation (17) can be expressed as follow:

$$\ln\left(F(\alpha)\right) = \ln t + \ln A - \frac{E}{R \cdot T},$$
(18)

where

$$\begin{cases} f(\alpha) = \alpha^m \cdot (1-\alpha)^n \\ F(\alpha) = \int_0^a \frac{d\alpha}{f(\alpha)} \end{cases} .$$
(19)

Usually, the glass substrate is temperature sensitive, so the bonding temperature during the COG packaging should be controlled accurately.

For the non-isothermal curing process, characterized by the heating rate β, the equation (13) can be rearranged as:

$$\frac{d\alpha}{dt} = \frac{d\alpha}{dT} \cdot \frac{dT}{dt} = \beta \cdot \frac{d\alpha}{dt} = A \cdot \exp\left(-\frac{E}{R \cdot T}\right) \cdot f(\alpha)$$
(20)

By integrating equation (20), the relationship of curing degree and curing temperature for certain heating rate can be given. According reference (Ozawa, 1970), the integral equation (20) can be expressed by means of polynomial form, i.e.

$$\lg \beta = \lg\left(\frac{A \cdot E}{R}\right) - \lg\left(F(\alpha)\right) - 2.32 - 0.457 \times \frac{E}{R \cdot T} .$$
(21)

For the isothermal curing of the ACF tested, taking activation energy, frequency factor as well as the coefficients m and n into equation (18), the function of cure degree is written as:

$$\ln\left(\int_0^a \frac{d\alpha}{\alpha^{1.06} \cdot (1-\alpha)^{0.94}}\right) = \ln\left(1.60 \times 10^8 \cdot t\right) - \frac{9.16 \times 10^3}{T}$$
(22)

Herein, t is curing time with the unit second, T is curing temperature with the unit K, and α is curing degree. Through the equation (22), the bonding time necessary to reach certain cure degree can be determined for certain bonding temperature. Figure 10 shows some typical relationship curves of curing temperature and time to reach some certain curing degree. It is found that for each curing degree, the curing time needed is lengthened with the temperature increasing of the isothermal curing process. Herein, some typical valuepairs for the curing time and temperature is chosen for the optimum curing degree range, i.e. 82%~85%, and listed in table 5.
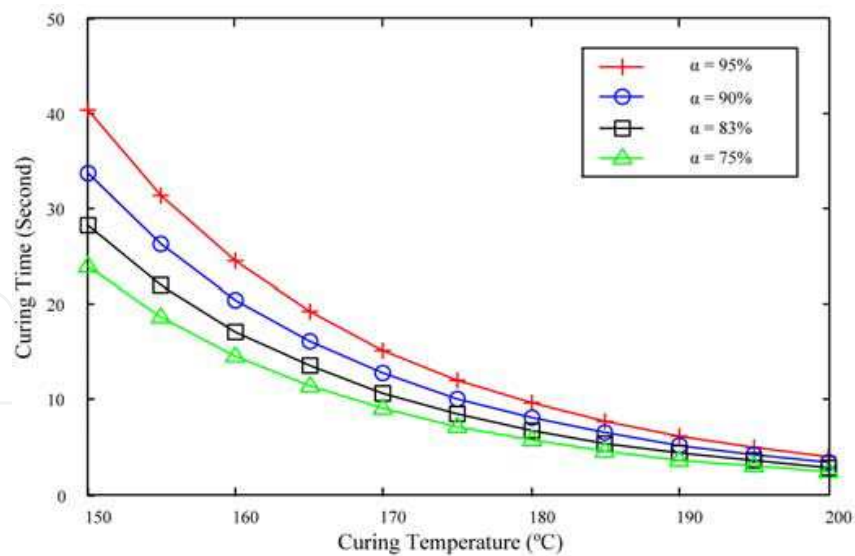
ACF Curing Process Optimization for Chip-on-Glass (COG)
Considering Mechanical and Electrical Properties of Joints
205

Fig. 10. Relationship of curing temperature versus time to reach some certain curing degrees

	Curing Degrees											
	82%			83%			84%			85%		
T (°C)	160	165	170	160	165	170	160	165	170	160	165	170
t (sec)	16.8	13.2	10.4	17.2	13.5	10.6	17.6	13.8	10.9	18.0	14.1	11.1

Table 5. Some typical value-pairs of curing temperature and time to reach certain curing degree in the recommended optimum range

5. Conclusions

In the work, the ACF curing process is optimized from the viewpoint of curing degree to find out the desirable curing process parameters. First of all, the influence of various curing degrees on the contact resistance of ACF joints is studied, using a systematic joints reliability evaluation method through some typical high hygrothermal fatigue tests. Degradation analysis is achieved, instead of the traditional failure time analysis, and the dependence of ACF joints' mean time to degradation on curing degree is analyzed, by which the optimum curing degree value as well as the recommend range is suggested. Results show that the optimum value for curing degree is 83% and the recommend range is from 82% to 85% for the ACF tested considering 95% confident interval. After that, the recommened curing parameters to reach certain desirable curing degree are also investigated, which is achieved by building the curing kinetics model of the ACF tested. The study of this work will provide an important support to optimize the curing process for various ACF-based packaging applications, such as the COG packaging for LCD, flip-chip bonding of radio frequency chips, and so on COG.

6. Acknowledgement

7. References

Boey, F.Y.C.; Qiang, W. (2000). Experimental modeling of the cure kinetics of an epoxyhexaanhydro- 4-methylphthalicanhydride (MHHPA) system. Polymer, Vol.41, 2081- 2094, 0032-3861

Chan, Y.C.; Uddin, M.O.; Chan, H.P. (2003). Curing Kinetics of Anisotropic Conductive Adhesive Film, *Journal of Electronic Materials*, Vol. 32, No. 3, 2003, 131-136

Chung, C.K,; Kwon, Y.M.; et al. (2008). Theoretical Prediction and Experimental Measurement of the Degree of Cure of Anisotropic Conductive Films (ACFs) for Chip-On-Flex (COF) Applications. *Journal of Electronic Materials*, Vol. 37, No. 10

Helge, K.; Liu, Johan (1998). Overview of Conductive Adhesive Interconnection Technologies for LCD's. IEEE Trans. on Components, Packaging, and Manufacturing Technology – Part A, Vol.21, No.2, 208-214, 1070–9886

Hwang, J.S.; Yim, M.J.; Paik, K.W. (2008). Effects of bonding temperature on the properties and reliabilities of anisotropic conductive films (ACFs) for flip chip on organic substrate application. *Microelectronics Reliability*, Vol. 48, 293-299, 0026-2714

Jarmo, M. (2003). Contact resistance of metal-coated polymer particles used in anisotropical conductive adhesives. Soldering & Surface Mount Technology,12–15, 0954-0911

Kim, J.W.; Kim, D.G; et al. (2008), Analysis of Failure Mechanism in Anisotropic Conductive and Non-Conductive Film Interconnections. *IEEE Trans. on Components and Packaging Technologies,* Vol. 31, No. 1, 65-73, 1521-3331

Lee, J.Y.; Shim, M.J.; Kim, S.W. (1997). Autocatalytic cure kinetics of natural zeolite filled epoxy composites. *Materials Chemistry and Physics*, Vol.48, 36-40, 0254-0584

Lin, Y. C.; Zhong Jue (2008). A review of the influencing factors on anisotropic conductive adhesives joining technology in electrical applications. *J. Material Science*, Vol. 43, 3072–3093

Masahiro I.; Katsuaki S. (2006). Effect of curing conditions on the electrical properties of isotropic conductive adhesives composed of an epoxy-based binder. *Soldering & Surface Mount Technology*, Vol.18, No.2, 40–45, 0954-0911

Myung J.Y.; Kyung W.P. (2006). Recent advances on anisotropic conductive adhesives (ACAs) for flat panel displays and semiconductor packaging applications. *Int. Journal of Adhesion & Adhesives*, Vol.26, 304-313, 0143-7496

Ozawa, T. (1970). Kinetic analysis of derivative curves in thermal analysis. *J. Thermal Analysis*, Vol.2, 301-324

Uddin, M.A.; Alam, M.O. et al. (2004). Adhesion strength and contact resistance of flip chip on flex packages –– effect of curing degree of anisotropic conductive film. *Microelectronics Reliability*, Vol. 44, 505–514, 0026-2714

Wu, C.M.; Chau, M.L. (2002). Degradation of flip-chip-on-glass interconnection with ACF under high humidity and thermal aging. *Soldering and Surface Mount Technology*, Vol. 14, No.2, 51–58, 0954-0911

Yim, M.J.; Jeong, I.H.; et al. (2005). Flip Chip Interconnection with Anisotropic Conductive Adhesives for RF and High-Frequency Applications. *IEEE Trans. on Components and Packaging Technologies,* Vol. 28, No. 4, 789-796, 1521-3331
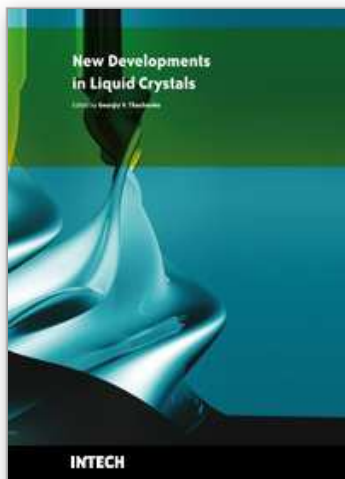
New Developments in Liquid Crystals

Edited by Georgiy V Tkachenko

Liquid crystal technology is a subject of many advanced areas of science and engineering. It is commonly associated with liquid crystal displays applied in calculators, watches, mobile phones, digital cameras, monitors etc. But nowadays liquid crystals find more and more use in photonics, telecommunications, medicine and other fields. The goal of this book is to show the increasing importance of liquid crystals in industrial and scientific applications and inspire future research and engineering ideas in students, young researchers and practitioners.

How to reference

In order to correctly reference this scholarly work, feel free to copy and paste the following:

Bo Tao, Han Ding, Zhouping Yin and Youlun Xiong (2009). ACF Curing Process Optimization for Chip-on-Glass (COG) Considering Mechanical and Electrical Properties of Joints, New Developments in Liquid Crystals, Georgiy V Tkachenko (Ed.), ISBN: 978-953-307-015-5, InTech, Available from: http://www.intechopen.com/books/new-developments-in-liquid-crystals/acf-curing-process-optimization-for-chip-on-glass-cog-considering-mechanical-and-electrical-properti

INTECH
open science | open minds